

# HIGH-GRADIENT TESTS ON AN S-BAND ACCELERATING STRUCTURE

Y. Igarashi<sup>†</sup>, S. Yamaguchi, Y. Higashi, A. Enomoto, T. Oogoe, K. Kakihara, and S. Ohsawa,  
KEK, 1-1 Oho, Tsukuba, Ibaraki, 305-0801 Japan

## Abstract

The accelerating gradient of an electron linac is limited by rf breakdown in the accelerating structure. An improvement of the breakdown limit is therefore necessary for the future upgrade of the KEKB injector linac as well as the linear collider. High-power tests were performed on a conventional S-band 2m-long accelerating structure for the KEKB injector linac. An average accelerating gradient of 40 MV/m and a field-enhancement factor of 53 were obtained after conditioning with  $1 \times 10^8$  rf shots.

We are examining the optimization of the high-pressure ultrapure water rinsing technique (HPR) condition for an S-band 2m-long accelerating structure. It was found that HPR can reduce dust particles to 1/10 or less on a disk surface.

## 1 HIGH-POWER TEST OF THE ACCELERATING STRUCTURE

### 1.1 Tested structure

The relevant parameters of the tested structure are given in Table 1 and Figure 1. The characteristics of this structure are as follows:

- (1) The disks and cylinders are machined by a high-precision turning lathe with a diamond byte.
- (2) The electroplating fabrication method is applied. The advantages of this method are:
  - a. The cavities are joined without adding heat at over 40 °C after machining. Therefore, the copper maintains a higher tensile strength.
  - b. Frequency tuning after electroplating is not required.
- (3) There is a crescent-shaped cut at the opposite side of the waveguide iris to correct the asymmetry of the electromagnetic fields in coupler cavities.

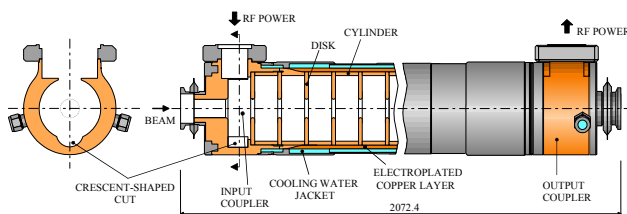


Figure 1: Schematic of the accelerating structure.

### 1.2 High-power test stand

We constructed a test stand for high-power tests of the

Table 1: Parameters of the tested accelerating structure.

Frequency	2856	MHz
Phase shift per cell	$2\pi / 3$	
Type of construction	Quasi-constant gradient	
Structure length	1889	mm
Number of cell	54	
Iris diameter $2a$	23.75 – 19.70	mm
Average shunt impedance	58.3	M $\Omega$ /m
Filling time	0.566	$\mu$ sec
Average group velocity $v_g/c$	0.0113	

accelerating structures (Figure 2). The maximum peak power of the klystron is 45 MW, and a SLED-type pulse compressor is installed.

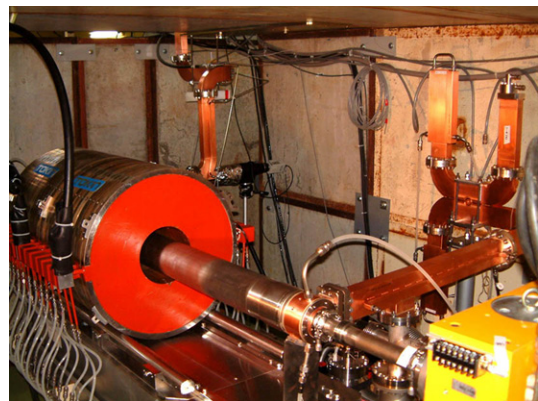


Figure 2: High-power test stand.

### 1.3 Experimental results

The pulse width and repetition rate of the rf pulse were 4.0  $\mu$ sec and 50 Hz, respectively, and the klystron output power load gradually increased. The reflection of the rf power from the accelerating structure or waveguides, and the vacuum pressure of the ion pumps were used as an interlock. The vacuum pressure of the accelerating structure was maintained at around  $1 \times 10^{-6}$  Pa during rf conditioning.

At first, a test was carried out with the SLED detuned. An average accelerating field of 20 MV/m was obtained after  $1.5 \times 10^7$  shots (54 hours). This test, however, was terminated because of a large reflection of the rf power to the klystron. After a 20 liter/sec ion pump was added to the klystron output, an average accelerating field of 23 MV/m was obtained after  $4.7 \times 10^7$  shots (the total number was  $6.2 \times 10^7$  shots (314 hours)). Next, a test was carried out with the SLED tuned, and an average accelerating field of 40MV/m was obtained after  $4.1 \times 10^7$  shots (The total number was  $1.0 \times 10^8$  shots (542 hours)). Also, the high-power test was terminated due to a time limit. The

<sup>†</sup>yasuhito.igarashi@kek.jp

average accelerating field (SLED tuned) versus the number of shots is shown in Figure 3.

The total amount of dark currents caused by field-emitted electrons load measured as an index of progress of the rf processing by two Faraday cups set upstream and downstream of the accelerating structure. The field-enhancement factor ( $\beta$ ) can be obtained from a modified Fowler-Nordheim (F.N.) plot. The F. N. plots and  $\beta$  values are shown in Figures 4 and 5, respectively. The final values of  $\beta$  (with SLED tuned,  $E=40$  MV/m) were 52 (upstream) and 53 (downstream), respectively.

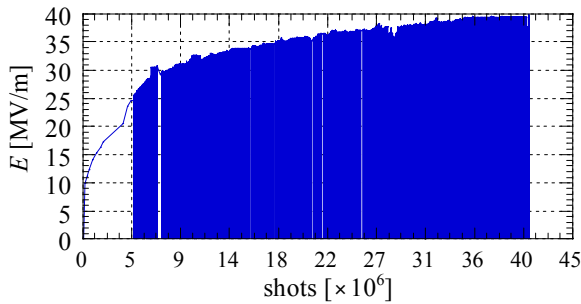


Figure 3: Average field vs. number of shots (with the SLED tuned).

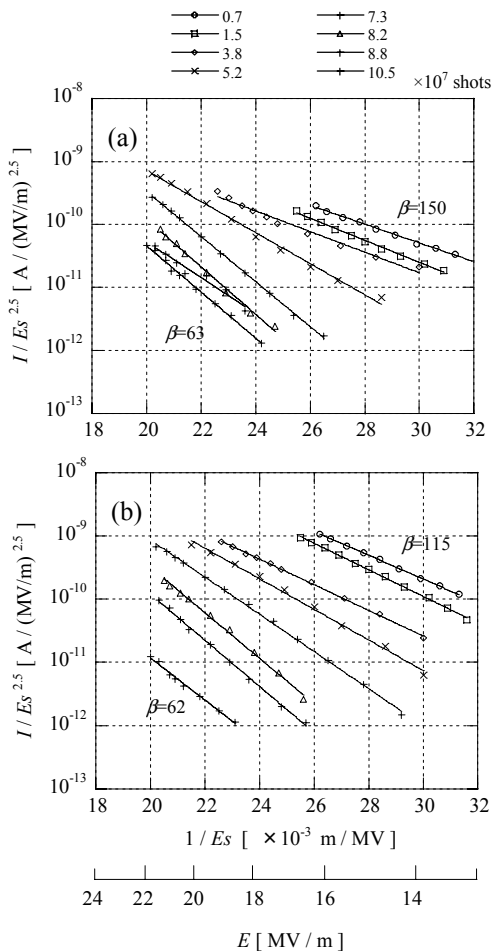


Figure 4: Modified F. N. plot (with the SLED detuned): (a) upstream, (b) downstream.

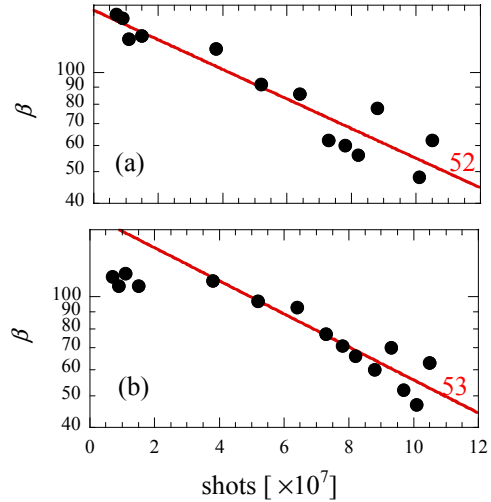


Figure 5: Field-enhancement factor ( $\beta$ ) vs. number of shots: (a) upstream, (b) downstream.

## 2 HIGH-PRESSURE ULTRAPURE WATER RINSING OF THE ACCELERATING STRUCTURE

It has been reported that the high-pressure ultrapure water rinsing technique (HPR) is very effective to improve the field gradients for normal conducting and superconducting RF cavities [1, 2]. HPR eliminates surface contamination, such as dust particles, that is thought to be one of the causes of field emission. We have a plan to apply this technique to the S-band 2m-long disk-loaded accelerating structure.

### 2.1 Removal effect of dust particles by HPR

We investigated the HPR effect on the surface of sample copper disks that were used with the accelerating structure. We measured the number and size of dust particles on a disk surface with a scanning electron microscope (SEM). Ultrapure water is pressurized up to 9MPa by a diaphragm pump, and is jetted from the nozzle of a stainless-steel pipe (Figure 6). A sample disk is set inside the stainless-steel vessel (Figure 7). This vessel turns around the pipe and moves up and down during water rinsing. After water rinsing, the vessel is dried by a scroll pump. A typical SEM photograph is shown in Figure 8.



Figure 7: Sample disk.

Figure 6: Nozzle of a stainless-steel pipe.

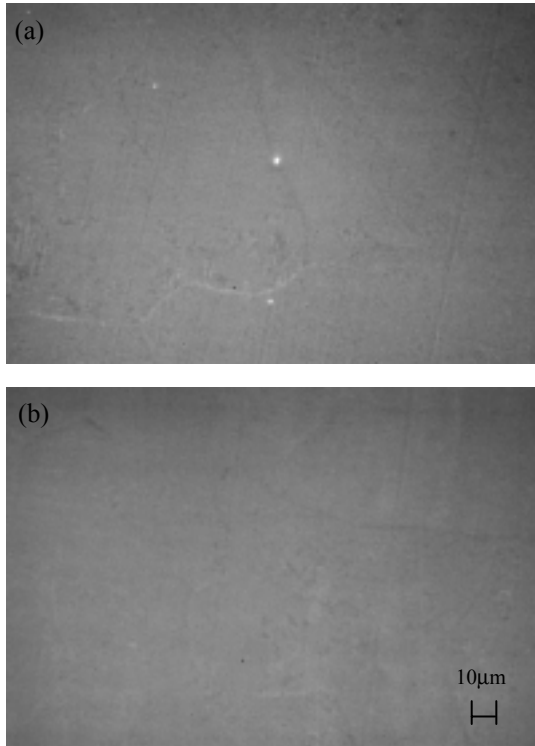


Figure 8: Typical surface of a copper disk: (a) before HPR, (b) after HPR

Figure 9 compares the results of the measured number and size of particles before and after HPR. The pump pressures were 3.0, 5.5 and 8.0 MPa and the rinsing times were 6, 15 and 30 min. It was found that HPR could reduce particles to 1/10 or less.

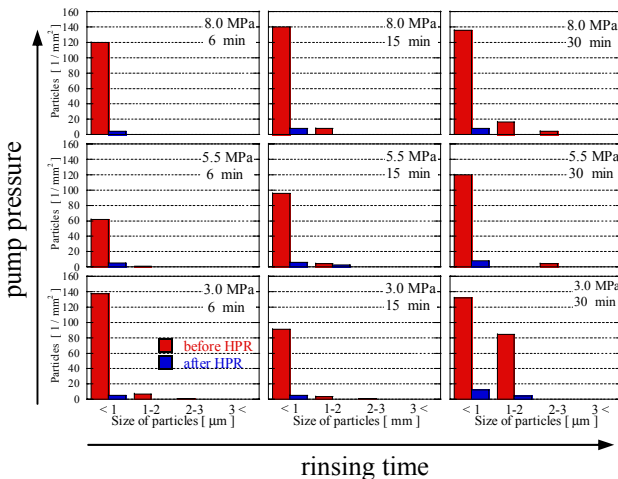


Figure 9: Comparison of the particle number and size for before and after HPR.

## 2.2 Optimization of the HPR condition

A surface analysis and observation of dust particles on disks will be performed using test cavities (acrylic model and copper model) to optimize the HPR condition before rinsing the 2m-long accelerator structure (Figure 10).

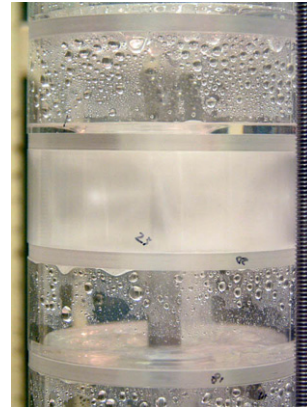


Figure 10: Acrylic model.

## 2.3 HPR of the S-band 2m-long disk-loaded accelerating structure

The HPR process of the S-band 2m-long disk-loaded accelerating structure is as follows. The accelerating structure is set up vertically and turns around the pipe and moves up and down during water-rinsing. First, the lower half of the accelerating structure is rinsed; next, it is reversed and the remaining half is rinsed.

After HPR, it is dried by a scroll pump immediately and various kinds of valves are attached in a clean room. After that, it is exhausted sufficiently by a turbo molecular pump and inserted in a high-power test stand. It is not exposed to the atmosphere after assembly in the clean room.

## 3 SUMMARY AND FUTURE

A high-power test was performed in an S-band 2m-long accelerating structure. An average accelerating field of 40 MV/m and the field enhancement factor ( $\beta$ ) of 53 were obtained after  $1.05 \times 10^8$  shots.

We apply the HPR to the whole part of an S-band 2m-long accelerating structure, and carry out a high-power test.

## 4 ACKNOWLEDGMENT

The authors wish to thank the members of the KEKB Injector for their help. We also acknowledge Dr. K. Saito for advice about the HPR and Dr. T. Higo for offering the stainless-steel vessel.

## 5 REFERENCES

- [1] K.Saito et al., "Study of Ultra-clean Surface for Niobium SC Cavities", Proceedings of the 6th Workshop on Superconductivity, 4-8 October, 1993, CEBAF, Newport News, USA, p.1151-1159.
- [2] M.Yoshioka et al., "High Gradient Studies on UHV Room Temperature Cavities at S-band for Linear Colliders", Proceedings of the 17th International Linac Conference, 1994, Tsukuba, Japan, p.302-304.